Brain Hallucination

François Rousseau

LSIIT, UMR CNRS/ULP, Strasbourg, France

Abstract. In this paper, we investigate brain hallucination, or generating a high resolution brain image from an input low-resolution image, with the help of another high resolution brain image. Contrary to interpolation techniques, the reconstruction process is based on a physical model of image acquisition. Our contribution is a new regularization approach that uses an example-based framework integrating non-local similarity constraints to handle in a better way repetitive structures and texture. The effectiveness of our approach is demonstrated by experiments on realistic Magnetic Resonance brain images generating automatically high-quality hallucinated brain images from low-resolution input.

1 Introduction

In medical imaging, a so-called low resolution 3D image is a stack of 2D thick slices. As a result, 3D data are generally not isotropic. This paper describes a method to reconstruct a 3D image that has a higher spatial resolution than the original image. In medical imaging, this is usually done by applying interpolation techniques [11], which can be divided into two groups: scene-based and object-based methods [10]. Scene-based approaches use only image intensities to determine the interpolated intensity (for instance: nearest neighbor, linear interpolation, spline-based interpolation). Such scene-based methods produce perceptually unsatisfactory results with blurred edges and textures. Many edge-preserving interpolation techniques have been reported to handle this problem. However, these techniques rely on accurate edge information that is not obtainable from coarse data. In order to guide the interpolation process, object-based methods make use of additional information extracted from images. An example of an object-based method is the registration-based approach where non-rigid registration is used to register adjacent slices, and then interpolation is carried out between corresponding positions in each slice [8], [14]. However, scene-based and object-based techniques do not take advantage of a model of the imaging process.

Another approach for image up-sampling is the model-based technique which relies on modeling the imaging processes and using regularization methods describing *a priori* constraints. This approach is related to super-resolution (SR) whose the purpose is to combine low resolution (LR) images to produce an image that has a higher spatial resolution than the original images [3]. In medical imaging, several SR methods have been proposed to combine LR images to reconstruct one HR image [15]. SR is a large research field encompassing many

D. Forsyth, P. Torr, and A. Zisserman (Eds.): ECCV 2008, Part I, LNCS 5302, pp. 497–508, 2008.

applications. The work we describe in this paper is related to single-frame SR [16], meaning that one LR image is used to generate a high resolution (HR) image. More specifically, we focus on studies involving Magnetic Resonance (MR) imaging for which an anatomical HR image and several other LR images are acquired to keep acquisition time at an acceptable level for the patient (see Figure 1). This is the case for many MR acquisitions performed in routine such as follow-up of multiple sclerosis disease, brain tumor evolution or diffusion tensor imaging. Typically, one isotropic HR T1-weighted image and several anisotropic LR images (such as T2-weighted, FLAIR or proton density images) are acquired. In this context, we propose a new method which uses information from a HR image to aid in the image magnification of a LR image.

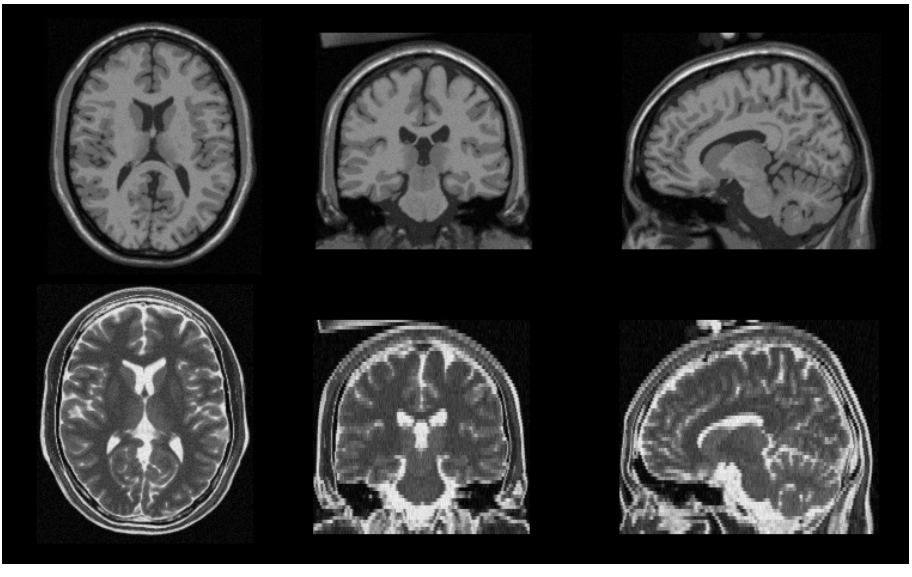

Fig. 1. Example of MR data [5]. First row: high resolution T1-weighted image ($1mm$ slice thickness); second row: low resolution T2-weighted image ($3mm$ slice thickness). The purpose of the method is to reconstruct a high-resolution T2-weighted image using information from the T1-weighted image.

2 Image Magnification

In this section, we present the model-based framework for image magnification which leads to an ill-posed inverse problem. Then, recently proposed regularization approaches relying on the example-based methodology are described.

2.1 Model-Based Framework

Contrary to interpolation approaches, we model the physical problem as in SR framework and the reconstructed image is obtained by inverting this problem. Model-based approaches use a generic observation model such as:

$$\mathbf{y} = DBW\mathbf{x} + \mathbf{n} \tag{1}$$

where $\mathbf{y}$ denotes the LR image, $\mathbf{x}$ is the high resolution (HR) image, $\mathbf{nr}$ represents observation noise, D is the subsampling matrix, B a blur matrix, W is the geometric transformation.

The three operators can be combined into a single matrix H: $H = DBW$. The matrix H thus incorporates motion compensation, degradation effects, and sub-sampling for the LR image $\mathbf{y}$. In this paper, we assume that the degradation operator H and the noise characteristics are known.

Based on this model, the SR image can be estimated by minimizing a least-square cost function such as:

$$\hat{\mathbf{x}} = \arg\min_{\mathbf{x}} \|\mathbf{y} - H\mathbf{x}\|^2 \ . \tag{2}$$

For such inverse problem, some form of regularization plays a crucial role and must be included in the cost function to stabilize the problem or constrain the space of solutions. Thus, the HR image is computed by considering the following equation:

$$\hat{\mathbf{x}} = \arg\min_{\mathbf{x}} \mathcal{L}(\mathbf{x}, \mathbf{y}, H) + \lambda\mathcal{R}(\mathbf{x}). \tag{3}$$

$\mathcal{L}(\mathbf{x}, \mathbf{y}, H)$ is a data fidelity term related to the physical model that penalizes inconsistency between the estimated HR image $\mathbf{x}$ and the observed LR image $\mathbf{y}$. $\mathcal{R}(\mathbf{x})$ is a regularization term. A common approach for regularization is to take explicitly into account the image geometry and to introduce a global weight λ that balances the contribution of prior smoothness terms and a fidelity term. Examples of pixel-based regularizers are Tikhonov regularization, Markov random field *a priori* image model or total variation.

However, there are two major drawbacks of pixel-based regularization methods: 1) there is no satisfying way to estimate the smoothing or regularization parameters from data, 2) generic smoothness priors may help regularize the problem, but cannot replace the missing information.

2.2 Example-Based Methods

To develop better image reconstruction algorithms, explicit models for the many regularities and geometries seen in local patterns are needed. In contrast to the pixel-based regularization approach, example-based methods consists in modeling non-local pairwise interactions from training data or a library of image patches. The principle of example-based SR methods is to add a similarity constraint between the voxels of HR image and the nearest examples present in the learning database [2],[7]. Such approach suggests that the reconstructed image should locally look like examples existing in the learning database. The regularization term can then be defined in a general way as follows:

$$\mathcal{R}(\mathbf{x}, \mathcal{E}) = \sum_{\mathbf{v},\mathbf{k}\in\Omega(\mathbf{v})} w_{\mathbf{v},\mathbf{k}} \|f(\mathbf{x}(\mathbf{v})) - \mathcal{E}_{\mathbf{v},\mathbf{k}}\|^2 \tag{4}$$

where $f(\mathbf{x}(\mathbf{v}))$ is an operator on the HR image $\mathbf{x}$ at the voxel $\mathbf{v}$, $\Omega(\mathbf{v})$ is a neighborhood of $\mathbf{v}$, $\mathcal{E}$ is the learning database, $\mathcal{E}_{\mathbf{v},\mathbf{k}}$ is a element of $\mathcal{E}$ related to $\mathbf{v}$ and $w_{\mathbf{v},\mathbf{k}}$ is a local weight. It is important to note that in example-based methods the regularization term $\mathcal{R}$ depends on the learning database $\mathcal{E}$.

Baker *et al.* in [2] have proposed a recognition-based gradient prior which enforces the constraints that the gradient of the HR image should be equal to the gradient of the best matching training image. The similarity constraint is then computed on image gradient values between each pixel of HR image and the best matching pixel in the learning database. In Equation 4, $f(\mathbf{x}(\mathbf{v}))$ would stand for the gradient value of the SR image $\mathbf{x}$ at the voxel $\mathbf{v}$ and $\mathcal{E}_{\mathbf{v},\mathbf{k}}$ would be the gradient value of the best matching pixel with respect to $\mathbf{v}$ in the learning database. Recently, Datsenko *et al.* in [7] have proposed another example-based regularization approach suggesting that the reconstructed image should agree with every found example and in every location. In this approach, $f(\mathbf{x}(\mathbf{v}))$ would be a patch of $\mathbf{x}$ centered in the voxel $\mathbf{v}$ and $\mathcal{E}_{\mathbf{v},\mathbf{k}}$ are the k nearest patches existing in the learning database.

In the context of face images, using a dedicated learning database, the problem of HR image reconstruction from a LR image has been investigated by Baker and Kanade [1]. This has been called *face hallucination* (see also [12]). Although the possibility to introduce new image priors makes the example-based approach very attractive, the key point (which can be a major drawback) is the need of a relevant learning database.

In this work, we proposed to take advantage of the MR imaging context and to investigate the use of a patch-based approach without any learning database by assuming that there exists related patterns in the LR anisotropic image and a HR isotropic image of the same patient.

3 Brain Hallucination

The purpose of this work is to reconstruct from one LR anistropic image with thick slices a HR isotropic brain image. In this context, we propose to use a patch-based approach to define the regularization term in order to take into account complex spatial interactions in images. Moreover, in contrast to example-based approaches for image modeling, the proposed method is unsupervised and thus uses no image patch learning database and no computational intensive training algorithms.

3.1 A New Regularization Term

The key idea of the proposed approach consists in saying that a HR image $\mathcal{E}_{\mathbf{x}}$ of a patient contains relevant examples which should be used to reconstruct a HR image $\mathbf{x}$ from a LR image $\mathbf{y}$ of the same patient and thus the HR image $\mathcal{E}_{\mathbf{x}}$ can be considered as a relevant candidate to be the learning database $\mathcal{E}$. We propose to introduce into the regularization term a similarity criterion between $\mathbf{x}$ and a patch-based regularized version of $\mathbf{x}$ using weights estimated from the HR image

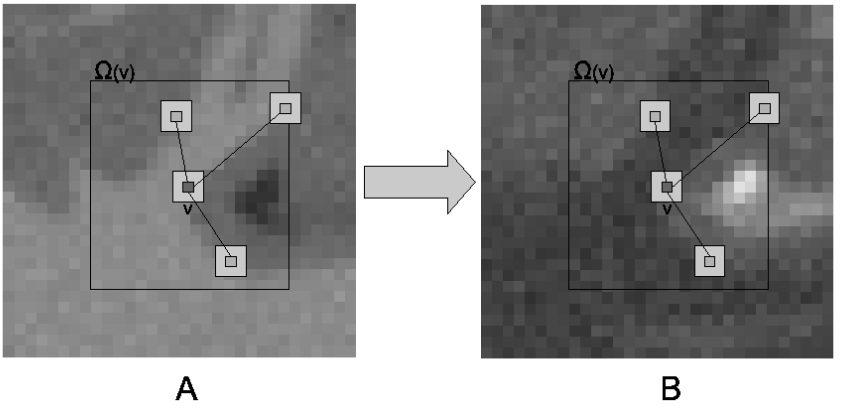

Fig. 2. Illustration of the regularization principle: the denoised value at voxel $\mathbf{v}$ in $\mathbf{x}$ is the weighted average of all intensities of voxels of $\mathbf{x}$ in the search volume $\Omega(\mathbf{v})$, based on the similarity of their intensity neighborhoods in the example HR image $\mathcal{E}_\mathbf{x}$. A) the example HR image $\mathcal{E}_\mathbf{x}$ is used to compute the weigths $w_{NLM}(\mathbf{v}, \mathbf{k}, \mathcal{E}_\mathbf{x})$. These weights describe local interactions between 3D patches. B) reconstructed HR image $\mathbf{x}$: weights $w_{NLM}(\mathbf{v}, \mathbf{k}, \mathcal{E}_\mathbf{x})$ estimated using the example HR image $\mathcal{E}_\mathbf{x}$ are used to estimated a regularized version of $\mathbf{x}$.

$\mathcal{E}_\mathbf{x}$. This regularization term can be seen as a similarity constraint between local patterns of $\mathbf{x}$ and $\mathcal{E}_\mathbf{x}$.

In the proposed approach, examples present in HR image $\mathcal{E}_\mathbf{x}$ are introduced in the regularization term by considering a denoised version of the HR image $\mathbf{x}$ obtained with a example-based framework. The proposed regularization term is defined as follows:

$$\mathcal{R}(\mathbf{x}, \mathcal{E}) = \sum_{\mathbf{v}} w_\mathcal{R}(\mathbf{v}) \|\mathbf{x}(\mathbf{v}) - d_{NLM}(\mathbf{x}(\mathbf{v}), \mathcal{E}_\mathbf{x})\|^2 \tag{5}$$

where $w_\mathcal{R}(\mathbf{v})$ is a local weight between data term $\mathcal{L}$ and regularization term $\mathcal{R}$. $d_{NLM}(\mathbf{x}(\mathbf{v}), \mathcal{E}_\mathbf{x})$ is a denoised (or regularized) version of $\mathbf{x}(\mathbf{v})$, estimated as follows:

$$d_{NLM}(\mathbf{x}(\mathbf{v}), \mathcal{E}_\mathbf{x}) = \sum_{\mathbf{k} \in \Omega(\mathbf{v})} w_{NLM}(\mathbf{v}, \mathbf{k}, \mathcal{E}_\mathbf{x}) \mathbf{x}(\mathbf{k}) \tag{6}$$

where $\Omega(\mathbf{v})$ corresponds to the neighborhood of the voxel $\mathbf{v}$ in the HR image $\mathbf{x}$. Figure 2 shows how example patterns in HR image $\mathcal{E}_\mathbf{x}$ are used to compute a regularized version of the reconstructed HR image $\mathbf{x}$. The use of a non-local approach to define the regularization term has the advantage over the PDE approach to handle in a better way repetitive structures and texture. As far as we know, our approach is the first one using a non-local operator for regularization to constraint the reconstruction process.

Our work is related to the Non Local Means (NLM) method introduced by Buades *et al.* in [4] for image denoising and recently applied for MRI denoising by Coupé *et al.* [6]. Buades *et al.* have shown that, for 2D natural images, the NLM

filter outperforms state-of-the-art denoising methods such as the Rudin-Osher-Fatemi Total Variation minimization scheme or the Perona-Malik Anisotropic diffusion. In the NLM algorithm, the restored intensity of the voxel $\mathbf{v}$, $NLM(\mathbf{v})$, is a weighted average of all voxel intensities in the image I:

$$NLM(\mathbf{v}) = \sum_{\mathbf{k} \in I} w_{NLM}(\mathbf{v}, \mathbf{k}) I(k) \tag{7}$$

where $I(\mathbf{k})$ is the intensity at voxel $\mathbf{k}$ and $w_{NLM}(\mathbf{v}, \mathbf{k})$ is the weight assigned to $I(\mathbf{k})$ in the restoration at voxel $\mathbf{v}$. The NLM method tries to take advantage of the high degree of redundancy of any natural image and appears to be an unsupervised example-based denoising method.

3.2 How to Deal with Outliers ?

The regularization term proposed in Equation 5 has been obtained by assuming that local patterns in the HR image $\mathcal{E}_{\mathbf{x}}$ could be used as examples to regularize the reconstructed HR image $\mathbf{x}$. However, there are some cases where this assumption may not hold. In the context of MR imaging, images $\mathcal{E}_{\mathbf{x}}$ and $\mathbf{y}$ are not acquired with the same MR sequence. Multimodal MR data do not reveal the same tissue specificity; for instance, Multiple Sclerosis (MS) lesions can be clearly visible in T2-weighted images but not in T1-weighted images (see Figure 3). In this case, the HR T1-weighted image may not be a relevant candidate to guide the reconstruction process. In order to handle the case of possible outliers, we propose to modify the regularization term by locally analyzing the correlation between two sets of local patterns.

To handle outliers, we propose another adaptive regularization term by modifying the way to compute the denoised version of the HR reconstructed image $\mathbf{x}$:

$$d_{NLM}(\mathbf{x}(\mathbf{v}), \mathcal{E}_{\mathbf{x}}) = \alpha \sum_{\mathbf{k} \in \Omega(\mathbf{v})} w_{NLM}(\mathbf{v}, \mathbf{k}, \mathcal{E}_{\mathbf{x}}) \mathbf{x}(\mathbf{k}) + (1-\alpha) \sum_{\mathbf{k} \in \Omega(\mathbf{v})} w_{NLM}(\mathbf{v}, \mathbf{k}, \mathbf{x}) \mathbf{x}(\mathbf{k}) \tag{8}$$

$d_{NLM}(\mathbf{x}(\mathbf{v}), \mathcal{E}_{\mathbf{x}})$ is now a weighted average of two denoised version of $\mathbf{x}(\mathbf{v})$. The first term is the denoised version of $\mathbf{x}(\mathbf{v})$ computed by using the HR image $\mathcal{E}_{\mathbf{x}}$ and the second term is also a denoised version of $\mathbf{x}(\mathbf{v})$ obtained with the current estimate of the reconstructed HR image $\mathbf{x}$. The weight α is defined as the correlation between the two set of weights $w_{NLM}(\mathbf{v}, \mathbf{k}, \mathcal{E}_{\mathbf{x}})$ and $w_{NLM}(\mathbf{v}, \mathbf{k}, \mathbf{x})$. If the weights are correlated, the HR image $\mathcal{E}_{\mathbf{x}}$ is likely to be a relevant candidate to guide the reconstruction process and thus, α is close to 1. If the weights are uncorrelated, the presence of outliers is detected and α is then close to 0. Defining $d_{NLM}(\mathbf{x}(\mathbf{v}), \mathcal{E}_{\mathbf{x}})$ in such way allows to choose the best examples to regularize the reconstructed HR image $\mathbf{x}$.

3.3 Computation of Weights w_{NLM}

Weights $w_{NLM}(\mathbf{v}, \mathbf{k}, \mathcal{E}_{\mathbf{x}})$ and $w_{NLM}(\mathbf{v}, \mathbf{k}, \mathbf{x})$ are computed in the same way. For the sake of clarity, we describe only the computation of $w_{NLM}(\mathbf{v}, \mathbf{k}, \mathcal{E}_{\mathbf{x}})$.

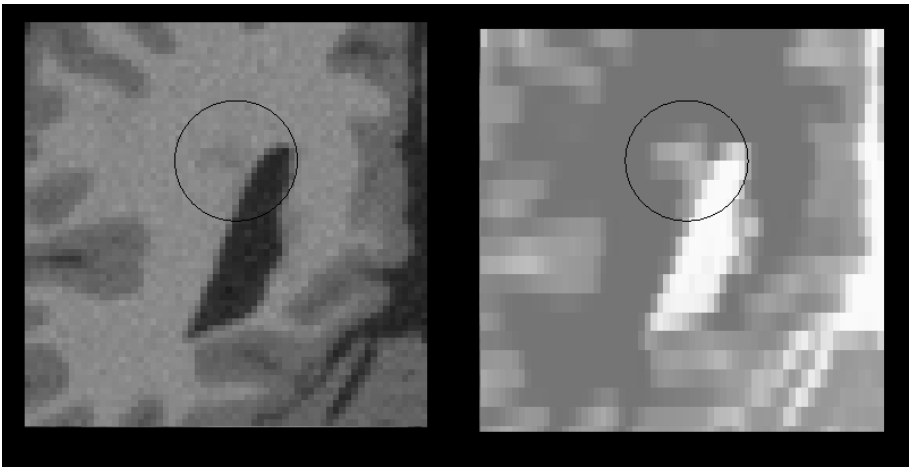

Fig. 3. Illustration of possible outliers. The MS lesion (in the circle) is less visible in the HR T1-weighted image than in the LR T2-weighted image. In this case, the assumption that local patterns in the HR image $\mathcal{E}_{\mathbf{x}}$ could be used as examples to regularize the reconstructed HR image $\mathbf{x}$ does not hold.

As in Coupé *et al.* [6], to reduce time computation, weight $w_{NLM}(\mathbf{v}, k, \mathcal{E}_{\mathbf{x}})$ is computed as follows:

$$w_{NLM}(\mathbf{v}, \mathbf{k}, \mathcal{E}_{\mathbf{x}}) = \frac{1}{Z_{\mathbf{v}}} e^{-\frac{\|P_{3D}(\mathcal{E}_{\mathbf{x}}(\mathbf{v})) - P_{3D}(\mathcal{E}_{\mathbf{x}}(\mathbf{k}))\|_2^2}{2\beta\hat{\sigma}^2|N_i|}} \tag{9}$$

where $P_{3D}(\mathcal{E}_{\mathbf{x}}(\mathbf{k}))$ is a 3D patch of HR image $\mathcal{E}_{\mathbf{x}}$ centered in voxel k and $P_{3D}(\mathcal{E}_{\mathbf{x}}(\mathbf{v}))$ is the 3D patch of HR image $\mathcal{E}_{\mathbf{x}}$ centered in voxel $\mathbf{v}$; $Z_{\mathbf{v}}$ is a constant of normalization. The distance between the 3D patches is the sum over voxels of patches of intensity differences using $L2$ norm. With the assumption on Gaussian noise (Equation 1), β is set to 1 (see [4] for theoretical justifications) and the standard deviation of noise is estimated via pseudo-residuals ϵ_v as defined in [9]. For each voxel $\mathbf{v}$ of HR image $\mathcal{E}_{\mathbf{x}}$, let us define:

$$\epsilon_v = \sqrt{\frac{6}{7}} \left(\mathcal{E}_{\mathbf{x}}(\mathbf{v}) - \frac{1}{6} \sum_{\mathbf{k} \in \Omega(\mathbf{v})} \mathcal{E}_{\mathbf{x}}(\mathbf{v}) \right) \tag{10}$$

where $\Omega(\mathbf{v})$ is the 6-neighborhood at voxel $\mathbf{v}$. The standard deviation of noise is computed as the least square estimator:

$$\hat{\sigma}^2 = \frac{1}{n} \sum_{k=1}^{n} \epsilon_k^2 \tag{11}$$

where n is the number of voxel in the HR image.

Moreover, as suggested by Mahmoudi and Sapiro in [13], voxel preselection can avoid useless computation and also improve the result of denoising. As in

[6], the preselection of relevant voxel is based on the mean and variance of 2D patches. $w_{\mathbf{v},k}$ is set to 0 if one of these conditions is not fulfilled:

$$\mu < \frac{\overline{P_{2D}(\mathbf{x}(\mathbf{v}))}}{\overline{P_{2D}(\mathbf{y}(\mathbf{k}))}} < \frac{1}{\mu} \tag{12}$$

$$\sigma^2 < \frac{var(P_{2D}(\mathbf{x}(\mathbf{v})))}{var(P_{2D}(\mathbf{y}(\mathbf{k})))} < \frac{1}{\sigma^2} \tag{13}$$

with $\mu = 0.95$ and $\sigma^2 = 0.5$.

3.4 Balance between Fidelity Data Term and Regularization Term

In Equation 3, λ is a global weight between fidelity data term and regularization term. This weight is usually tuned by error and trial since there is no satisfying way to estimate it. In our approach, λ is set to 1 and we propose a non-stationary approach by using local weights $w_{\mathcal{R}}(\mathbf{v})$ for each voxel $\mathbf{v}$ which are defined using the point spread function of the acquisition system as follows:

$$w_{\mathcal{R}}(\mathbf{v}) = \frac{1 - \sum_r b(\|\mathbf{v} - \mathbf{y}_r\|_2)}{\sum_r b(\|\mathbf{v} - \mathbf{y}_r\|_2)} \tag{14}$$

where b is the point spread function (b is related to the blur matrix B used in Equation 1). $w_{\mathcal{R}}(\mathbf{v})$ increases if the voxel $\mathbf{v}$ is far of LR image data.

4 Results

In each experiment, as suggested in [6], parameter values for patches are: search area $11 \times 11 \times 11$ voxels, patch size $3 \times 3 \times 3$ voxels. Moreover, a gradient descent method is used to optimize the cost function.

To explore the ability to reconstruct high resolution image of realistic typical anatomical brain structures, we applied the algorithm on MRI images of Brainweb [5]. Brainweb is a simulated brain database which is often used as a gold standard for the analysis of in vivo acquired data. The database contains simulated brain MRI data based on two anatomical models: normal and multiple sclerosis (MS lesions have been extracted from real MRI data). Using the HR image provided by Brainweb, we have generated low resolution images using the observation model described by Equation 1. Thus, the ground truth is available and it can be compared with the reconstructed HR brain images. Figures 4 and 5 show the results for pathological and non pathological MR Brainweb images for axial, coronal and sagittal views. We also reported PSNR in decibels (dB) results obtained with the different methods in Table 1.

$$PSNR = 10 \log_{10} \left(\frac{d^2}{|\Omega|^{-1} \sum_{\mathbf{v} \in \Omega} (\mathbf{x}(\mathbf{v}) - \hat{\mathbf{x}}(\mathbf{v}))^2} \right)$$

where d is the reference image dynamic. Results obtained with the proposed approach compare favorably with fifth-order B-spline interpolation. Fine details have been successfully recovered and contrast between structures has been improved.

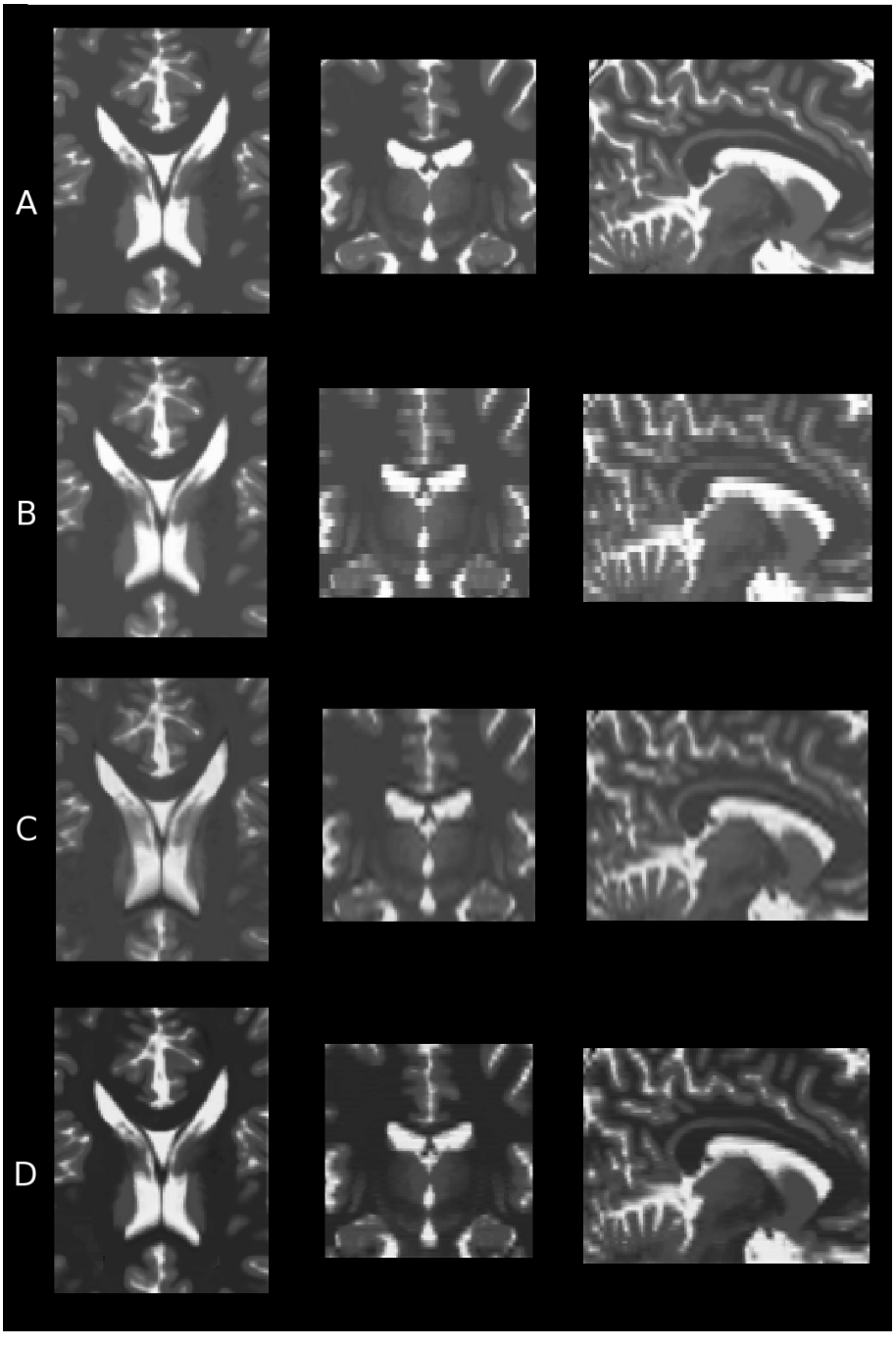

Fig. 4. Reconstruction results (non pathological case). A) Ground truth, B) input LR image, C) fifth order B-spline interpolation, D) the proposed approach.

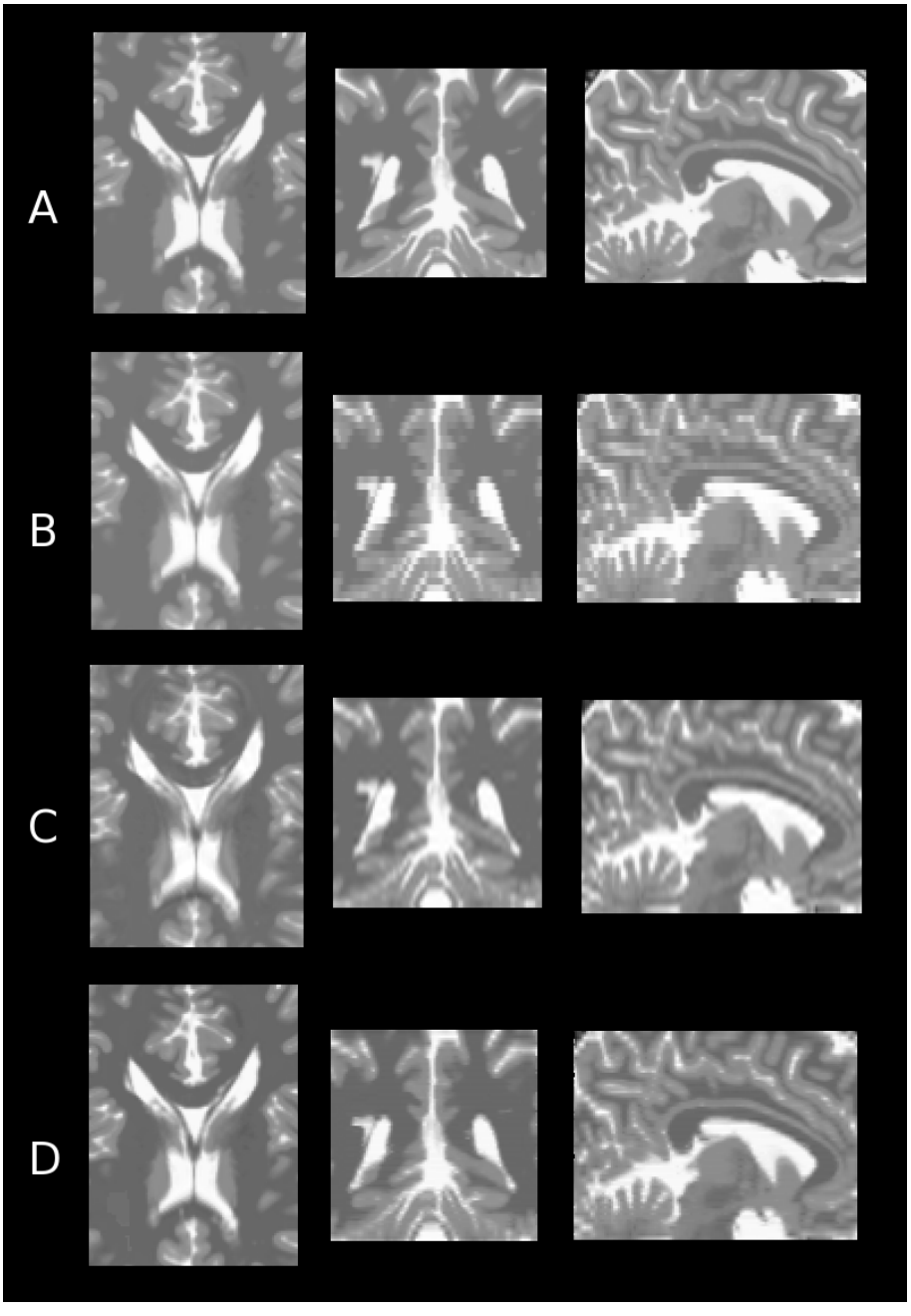

Fig. 5. Reconstruction results in presence of MS lesions. A) Ground truth, B) input LR image, C) fifth order B-spline interpolation, D) the proposed approach.

Table 1. Performances of image reconstruction methods

Method	Non pathological Image	Multiple Sclerosis Image
Nearest Neighbour Interpolation	23.26	26.11
Trilinear Interpolation	26.17	27.30
3rd order B-spline Interpolation	27.80	28.36
5th order B-spline Interpolation	27.93	28.48
Our method	28.24	29.75

5 Conclusion

We have shown that example-based approaches such as non-local means can be embedded into the reconstruction process to enhance the performance of super resolution techniques. If a HR brain image of the patient is available, LR images of the same patient can be enhanced by exploiting non-local pairwise interactions. Experimental results prove that the developed algorithm including an image acquisition model compares favorably with interpolation approach. High resolution imaging is a key point for MR brain image analysis in order to study anatomical details. Such HR image reconstruction algorithm represents an important step towards multimodal brain analysis at fine scale.

To develop better image reconstruction algorithms, example-based SR methods try to add a similarity constraint between the voxels of HR image and the nearest examples present in the learning database. In the medical context studied in this paper, the learning database contains only one HR image. Further work concerns the extension and application of this approach to other domains such as computational photography or image fusion, and also when no HR image example is available.

Acknowledgment

The research leading to these results has received funding from the European Research Council under the European Communitys Seventh Framework Programme (FP7/2007-2013 Grant Agreement no. 207667). The author would like to thank S. Faisan from LSIIT/University of Strasbourg for fruitful discussions.

References

1. Baker, S., Kanade, T.: Hallucinating Faces. In: Fourth Int. Conf. on Automatic Face and Gesture Recognition (2000)
2. Baker, S., Kanade, T.: Limits on Super-Resolution and How to Break Them. IEEE Trans. Pattern Analysis and Machine Intelligence 24(9), 1167–1183 (2002)
3. Bose, N.K., Chan, R.H., Ng, M.K.: Special Issue: High Resolution Image Reconstruction. Int. J. of Imaging Systems and Technology 14(2-3) (2004)
4. Buades, A., Coll, B., Morel, J.M.: A review of image denoising algorithms, with a new one. Multiscale Modeling & Simulation 4(2), 490–530 (2005)

5. Cocosco, C.A., Kollokian, V., Kwan, R.K.-S., Evans, A.C.: BrainWeb: Online Interface to a 3D MRI Simulated Brain Database. In: Proceedings of 3-rd International Conference on Functional Mapping of the Human Brain, vol. 5(4) (1997)
6. Coupé, P., Yger, P., Prima, S., Hellier, P., Kervrann, C., Barillot, C.: An Optimized Blockwise Non Local Means Denoising Filter for 3D Magnetic Resonance Images. IEEE Trans. Medical Imaging (2007)
7. Datsenko, D., Elad, M.: Example-based single document image super-resolution: a global MAP approach with outlier rejection. Multidim. Syst. Sign. Process 18, 103–121 (2007)
8. Frakes, D.H., Dasi, L.P., Pekkan, K., Kitajima, H.D., Sundareswaran, K., Yoganathan, A.P., Smith, M.J.T.: A New Method for Registration-Based Medical Image Interpolation. IEEE Trans. Medical Imaging 27(3), 370–377 (2008)
9. Gasser, T., Sroka, L., Steinmetz, C.: Residual variance and residual pattern in nonlinear regression. Biometrika 73(3), 625–633 (1986)
10. Grevera, G.J., Udupa, J.K.: An objective comparison of 3-D image interpolation methods. IEEE Transactions on Medical Imaging 17, 642–652 (1998)
11. Lehmann, T., Gonner, C., Spitzer, K.: Survey: Interpolation Methods in Medical Image Processing. IEEE Transactions on Medical Imaging 18(11), 1049–1075 (1999)
12. Liu, C., Shum, H.-Y., Freeman, W.T.: Face Hallucination: Theory and Practice. Int. Journal of Computer Vision 75(1), 115–134 (2007)
13. Mahmoudi, M., Sapiro, G.: Fast image and video denoising via nonlocal means of similar neighborhoods. IEEE Signal Processing Letters 12(12), 839–842 (2005)
14. Penney, G.P., Schnabel, J.A., Rueckert, D., Viergever, M.A., Niessen, W.J.: Registration-Based Interpolation. IEEE Transactions on Medical Imaging 23(7), 922–926 (2004)
15. Rousseau, F., Glenn, O., Iordanova, B., Rodriguez-Carranza, C., Vigneron, D., Barkovich, J., Studholme, C.: Registration-Based Approach for Reconstruction of High-Resolution in Utero Fetal MR Brain images. Academic Radiology 13(9), 1072–1081 (2006)
16. van Ouwerkerk, J.D.: Image super-resolution survey. Image and Vision Computing 24, 1039–1052 (2006)